tris-HCl, 100 mM potassium acetate, 200 mM KCl, 2.5 mM $MgCl_2$, 1 mM dithiothreitol (DTT)], followed by addition of stoichiometric amounts of 40S subunit and incubation at 37°C for 15 min. The final complex concentration was about 500 nM. The samples were snap-frozen with liquid nitrogen and stored at −80°C until use.

Samples of 40S subunits (final concentration about 50 nM) were applied to cryo-EM grids and shock-frozen in liquid ethane (*37*, *38*). Micrographs were recorded under low-dose conditions in a defocus range between 1.7 μm and 5.7 μm on a Philips F20 (FEI/Philips) at a magnification of 50.000 ± 2%. From the micrographs, 69 were selected for the vacant 40S subunit, 74 for the IRES-40S complex, and 61 for the IRESΔdII-40S complex. The micrographs were scanned on a Highscan drum scanner (Eurocore/Saint-Denis, France) with a resolution of 1069 dpi corresponding to a pixel size of 4.78 Å on the object scale. The data were analyzed using the SPIDER system (*39*). After automated particle preselection, manual verification, and selection by cross-correlation, 18,801 particles were chosen for the vacant 40S subunit, 20,939 particles for the IRES-40S complex, and 13,613 particles for the IRESΔdII-40S complex. The data sets were subdivided each into 16 to 23 defocus groups, and a refined, three-dimensional reconstruction that was corrected for the contrast transfer function was calculated for each of the 40S samples (*40*). The final resolution was estimated by the Fourier shell correlation with a cutoff value of 0.5. It is 22.7 Å for the vacant 40S subunit, 19.8 Å for the IRES-40S complex, and 21.9 Å for the IRESΔdII-40S complex. According to the more lenient (*17*) 3σ criterion (*41*), the resolution values would be 15.9 Å, 14.5 Å, and 15.4 Å, respectively.

16. S. Srivastava, A. Verschoor, M. Radermacher, R. Grassucci, J. Frank, *J. Mol. Biol.* **245**, 461 (1995).
17. A. Malhotra *et al.*, *J. Mol. Biol.* **280**, 103 (1998).
18. M. G. Gomez-Lorenzo *et al.*, *EMBO J.* **19**, 2710 (2000).
19. J. Frank *et al.*, *Nature* **376**, 441 (1995).
20. J. Frank *et al.*, *Biochem. Cell Biol.* **73**, 757 (1995).
21. To our knowledge, the ribosomal region at the back of the platform has not been previously implicated in molecular recognition of a ribosomal ligand. As does the protein conducting channel Sec61 (translocon) (*42*, *43*), the HCV IRES recognizes the evolutionarily more divergent outer surfaces of the ribosome. Thus, the surfaces available for specific molecular recognition extend beyond the highly conserved binding sites for tRNAs and elongation factors. The fact that the HCV IRES binds to the more variable regions of the 40S subunit surface may explain its ability to distinguish the 40S subunit of rabbit from that of wheat germ (*12*).
22. D. V. Sizova, V. G. Kolupaeva, T. V. Pestova, I. N. Shatsky, C. U. Hellen, *J. Virol.* **72**, 4775 (1998).
23. S. Srivastava, A. Verschoor, J. Frank, *J. Mol. Biol.* **226**, 301 (1992).
24. M. Honda, M. R. Beard, L. H. Ping, S. M. Lemon, *J. Virol.* **73**, 1165 (1999).
25. R. K. Agrawal *et al.*, *J. Cell Biol.* **150**, 447 (2000).
26. J. Frank *et al.*, *The Ribosome: Structure Function Antibiotics and Cellular Interactions*, R. A. Garrett *et al.*, Eds. (ASM Press, Washington, DC, 2000), p. 45.
27. An animated sequence showing the conformational change is available as supplementary material on *Science* Online at www.sciencemag.org/cgi/content/full/291/5510/1959/DC1.
28. C. M. Spahn, R. Beckmann, G. Blobel, J. Frank, unpublished observations.
29. C. M. T. Spahn, P. Penczek, A. Leith, J. Frank, *Structure Fold. Des.* **8**, 937 (2000).
30. A. P. Carter *et al.*, *Nature* **407**, 340 (2000).
31. K. R. Lata *et al.*, *J. Mol. Biol.* **262**, 43 (1996).
32. S. Waga, B. Stillman, *Annu. Rev. Biochem.* **67**, 721 (1998).
33. J. S. Kieft, K. Zhou, J. A. Doudna, unpublished observations.
34. Moreover, deletion of domain II strongly reduces an ultraviolet radiation-induced cross-link between the IRES RNA and ribosomal protein S9 (the homolog of bacterial protein S4) (*44*). Electron microscopy of antibody-labeled 40S subunits located S9 at the back of the shoulder, below helix 16, near the mRNA binding cleft entry site (*45*), in agreement with the placement of bacterial S4 within the 30S subunit (*2*, *3*, *46*). This position is quite far away from the structured part of the HCV IRES RNA in our density map, suggesting that the IRES RNA-S9 cross-link occurs to the coding part of the IRES RNA just 3′ of the start codon (*12*). Thus, the domain II–induced changes in the ribosome structure around the coding RNA, as well as the direct restriction of movement of the single-stranded coding part of the RNA by the terminal loop of domain II (see above), may explain the differing efficiencies of the S9-RNA cross-link between IRES RNA with and without domain II.
35. This would be consistent with toe-printing experiments that show a decrease in the intensity of the stop associated with mRNA bound in the cleft when domain II is removed (*44*). Removal of domain II also causes a slight change in the position of IRES RNA domain IIIb relative to the surface of the 40S subunit, although binding data show that the overall IRES RNA affinity for the 40S subunit remains unchanged and that there are no changes in ribosome structure in this region. The significance of this observation is presently not clear.
36. It is difficult to imagine domain II remaining in place during elongation, as this would restrict both coding RNA and ribosome movement; some mechanism must exist to release this contact. Perhaps once elongation has begun, tRNA moving into the E site during the translocation step might displace domain II, effectively releasing the ribosome from its IRES-induced conformation, opening up the entry site for incoming coding RNA, and allowing unrestricted ribosome movement during elongation. Alternatively, subunit association could move the 40S subunit out of its IRES-induced conformation, thus ejecting domain II from its contact point.
37. T. Wagenknecht, R. Grassucci, J. Frank, *J. Mol. Biol.* **199**, 137 (1988).
38. J. Dubochet *et al.*, *Q. Rev. Biophys.* **21**, 129 (1988).
39. J. Frank *et al.*, *J. Struct. Biol.* **116**, 190 (1996).
40. J. Frank, P. Penczek, R. K. Agrawal, R. A. Grassucci, A. B. Heagle, *Methods Enzymol.* **317**, 276 (1999).
41. E. V. Orlova *et al.*, *J. Mol. Biol.* **271**, 417 (1997).
42. R. Beckmann *et al.*, *Science* **278**, 2123 (1997).
43. J. F. Ménétret *et al.*, *Mol. Cell* **6**, 1219 (2000).
44. V. G. Kolupaeva, T. V. Pestova, C. U. Hellen, *J. Virol.* **74**, 6242 (2000).
45. G. Lutsch, H. Bielka, G. Enzmann, F. Noll, *Biomed. Biochim. Acta* **42**, 705 (1983).
46. W. M. Clemons Jr. *et al.*, *Nature* **400**, 833 (1999).
47. M. Carson, *J. Appl. Crystallogr.* **24**, 103 (1991).
48. This work was funded, in part, by grants from NIH (R37 GM29169 to J.F. and GM60635 to P.A.P) and NSF (DBI 9871347 to J.F.). We thank Y. Chen for assistance with the illustrations and R. T. Batey, P. Adams, and P. Masters for critically reading the manuscript.

18 December 2000; accepted 25 January 2001

A Proteolytic Transmembrane Signaling Pathway and Resistance to β-Lactams in Staphylococci

H. Z. Zhang, C. J. Hackbarth, K. M. Chansky, H. F. Chambers*

β-Lactamase and penicillin-binding protein 2a mediate staphylococcal resistance to β-lactam antibiotics, which are otherwise highly clinically effective. Production of these inducible proteins is regulated by a signal-transducing integral membrane protein and a transcriptional repressor. The signal transducer is a fusion protein with penicillin-binding and zinc metalloprotease domains. The signal for protein expression is transmitted by site-specific proteolytic cleavage of both the transducer, which autoactivates, and the repressor, which is inactivated, unblocking gene transcription. Compounds that disrupt this regulatory pathway could restore the activity of β-lactam antibiotics against drug-resistant strains of staphylococci.

β-Lactam antibiotics are the most effective drugs for the treatment of staphylococcal infections, yet they often cannot be used because many strains are resistant. Resistance is due to production of either β-lactamase or an extra penicillin-binding protein, PBP 2a (*1*, *2*). β-Lactamase, encoded by *blaZ*, inactivates penicillin by hydrolysis of its β-lactam ring. PBP 2a, encoded by the chromosomal gene *mecA*, in methicillin-resistant strains of staphylococci, confers resistance not only to penicillin, but also to all β-lactam antibiotics. PBP 2a, which is probably a transpeptidase (*3*), can substitute for other PBPs but, because of its low affinity for binding β-lactams, is unbound at clinically relevant concentrations of antibiotic, allowing cell wall synthesis to continue (*4*). Although β-lactamase and PBP 2a are genetically and biochemically distinct, both are regulated by similar sensor-transducer and repressor proteins. Their regulatory proteins are homologs of each other and of those controlling expression of inducible β-lactamase in *Bacillus licheniformis* (*5*–*7*). In staphylococci, the

Division of Infectious Diseases, San Francisco General Hospital, Department of Medicine, University of California at San Francisco, 1001 Potrero Avenue, San Francisco, CA 94110, USA.

*To whom correspondence should be addressed. E-mail: chipc@itsa.ucsf.edu

genes for the sensor-transducer (*blaR1* or *mecR* for β-lactamase or PBP 2a, respectively) and the DNA binding repressor protein (*blaI* or *mecI*) are located immediately upstream of the structural gene (*blaZ* or *mecA*) and are transcribed in the opposite direction as a polycistronic message. Repressor binds as a homodimer to palindromic sites within the *mec* and *bla* intergenic promoter regions, nucleotide sequences of which are 57% identical, blocking transcription of both structural and regulatory genes (*8–10*). Either *bla* or *mec* regulatory genes can control production of PBP 2a and β-lactamase because of the high degree of homology of the two systems (*8, 11*); although regulation in clinical isolates is principally by *bla* because of deletions or mutations in the *mec* regulatory genes that weaken repressor activity (*12, 13*).

β-Lactam binding to the extracellular, penicillin-binding domain of the sensor transducer generates a transmembrane signal that results in the removal of repressor from DNA binding sites, allowing for transcription of both structural and regulatory genes (*10, 14*). The details of this signaling mechanism have been a mystery. Induction of β-lactamase is accompanied by proteolysis of BlaI with conversion of 14-kD BlaI into an ~11-kD fragment (*10*). To determine its site of cleavage, we tagged BlaI with the 11–amino acid c-Myc sequence (*15–17*). Under inducing conditions, identically sized 11-kD BlaI fragments were detected in the *Staphylococcus aureus* transformants expressing wild-type BlaI or BlaI tagged at its COOH-terminus, indicating a COOH-terminal location of the cleavage site (Fig. 1A). Accordingly, BlaI tagged with c-Myc sequence at the NH_2-terminus generated a BlaI fragment that migrated more slowly than that of COOH-terminus–tagged BlaI (Fig. 1B).

The specific cleavage site within BlaI was located by engineering a construct where the glutathione *S*-transferase (GST) gene, *gst*, was fused in-frame to the COOH-terminus of *blaI* (*18*). The NH_2-terminal amino acid sequence of cleaved GST-BlaI fusion product was determined to be FAKNEELNN (*19*), which localized the site of cleavage between residues N^{101} and F^{102} residing within the sequence NH_2-KSLVL $N^{101}F^{102}$AKNEELNN. Substitution mutation of $A^{101}A^{102}$ for $N^{101}F^{102}$ (N101A, F102A) at this site both prevented proteolysis of BlaI (Fig. 1C) and inducible expression of β-lactamase (*20*). Thus, site-specific proteolytic cleavage of BlaI near its COOH-terminus is required for reversal of transcriptional repression in this signal transduction pathway.

BlaR1 is a prime candidate for the protease that cleaves BlaI. Deletion or mutation of *blaR1* prevents β-lactamase induction and proteolysis of BlaI (*10, 11*). In addition, a H^{201}EXXH zinc metalloprotease signature motif is present within the predicted 186–amino acid cytoplasmic domain (*14, 21*). The histidine residues of metalloproteases with this signature motif are essential for zinc binding, and the glutamic acid residue is a catalytic base (*22*). Two site-directed mutations, $His^{201} \rightarrow Ala^{201}$ (H201A) and $Glu^{202} \rightarrow Ala^{202}$ (E202A), were introduced into BlaR1. Either mutation prevented the cleavage of BlaI (Fig. 1D) and induction of β-lactamase.

Zinc metalloproteases typically are autocatalytic proenzymes activated by intramolecular cleavage (*23*). We have previously reported the presence of an inducible ~35-kD PBP in transformants of the methicillin-resistant strain COL containing intact *blaR1* but not in a transformant in which *blaR1* had been disrupted (*11, 24*), suggesting that the 35-kD PBP was a cleavage product of BlaR1. Cleavage of BlaR1 was confirmed by using antiserum against a synthetic peptide identical in sequence to that within the BlaR1 cytoplasmic domain (Fig. 2A). An inducible 33- to 35-kD peptide, as well as a small amount of a larger protein, corresponding to full-length 66-kD BlaR1 was detected in the transformant COL631.

The specific site at which BlaR1 is cleaved and the participation of the HEXXH motif in its proteolysis were investigated with a pair of *S. aureus* strain RN4220 transformants into which a COOH-terminus His^6-tagged BlaR1 fusion had been introduced. In one transformant, the zinc metalloprotease motif was wild-type, H^{201}EXXH, and in the other, a E202A substitution mutation had been introduced. An inducible, His^6-tagged 33-kD protein (but no 66-kD protein) was detected in the transformant containing intact HEXXH sequence but not in the transformant with the E202A mutation (Fig. 2B). Thus, the zinc metalloprotease signature motif of BlaR1 is not only required for the cleavage of BlaI, but also is required for its own cleavage.

The His^6-tagged 33-kD polypeptide was then purified from lysates of whole cells (*18*). Its NH_2-terminal amino acid sequence was determined to be RLINIKEAN, localizing the specific cleavage site within the sequence KKSLIKR^{293}RLINIKEA of the BlaR1 cytoplasmic domain. A transformant containing mutant BlaR1 [$Arg^{293} \rightarrow Ala^{293}$ (R293A)] did not degrade BlaI (Fig. 1E), and β-lactamase was not detectable under noninducing or inducing conditions. Thus, the signal initiating proteolysis of BlaI and release of repression also involves site-specific proteolysis of BlaR1.

To determine whether BlaR1 generation could be autocatalytic or required a staphylococcal co-factor, we cloned *blaR1* tagged at its 3′ end with a His^6 sequence (to monitor for cleaved gene products) under control of an isopropyl-β-D-thiogalactopyranoside (IPTG)–inducible promoter into a tightly regulated *Escherichia coli* expression vector. His^6-tagged peptides of ~19, 31 to 36, and 61 kD were expressed in the presence of IPTG (Fig. 3). The amount of the 31-kD peptide was relatively increased in the presence of the β-lactam inducer, 2-(2′-carboxyphenyl)benzoyl-6-aminopenicillanic acid (CBAP). These results are consistent with autocatalysis of BlaR1 triggered by binding of inducer.

The sequence of events during induction of β-lactamase appears to be as follows. Bacteria detect β-lactam antibiotic by its binding to the penicillin-binding domain of the sensor

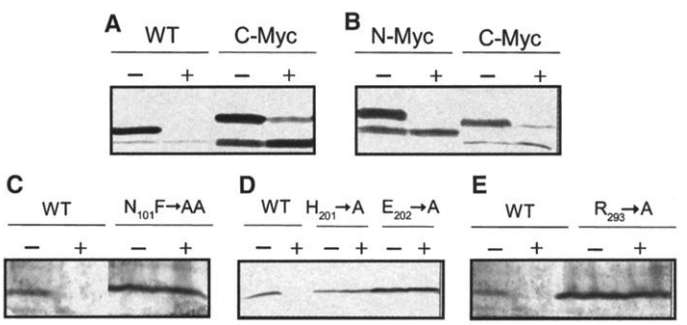

Fig. 1. Western blot analysis of BlaI in whole cells of *S. aureus* strain RN4220 transformants, grown under noninducing (–) and inducing (+) conditions (*29*). (**A** and **B**) WT is a transformant with pCH2278 (*11, 24*), which is a wild-type *bla* locus cloned into pRN5542 (*30*). C-Myc indicates the transformant with c-Myc sequence EQKLISEEDLN (*17, 19*) tagged onto the COOH-terminus of BlaI (*15, 16*), and N-Myc indicates that c-Myc sequence was tagged onto the NH_2-terminus of BlaI. (**C**) Lanes $N_{101}F \rightarrow AA$ indicate the transformant with these amino acid substitution mutations (N101A, F102A) introduced into BlaI. (**D**) Lanes $H_{201} \rightarrow A$ and $E_{202} \rightarrow A$ are transformants with these point mutations (H201A and E202A, respectively) introduced into the H^{201}EXXH zinc metalloprotease motif of BlaR1. (**E**) Lanes $R_{293} \rightarrow A$ are the transformant containing this substitution mutation (R293A) introduced into BlaR1. For induction of β-lactamase, log-phase organisms were grown in tryptic soy broth with and without CBAP (10 μg/ml). Cells were pelleted by centrifugation, resuspended in lysis buffer [lysostaphin (200 μg/ml), 10 mM $MgCl_2$, deoxyribonuclease (15 μg/ml), ribonuclease (15 μg/ml), and 20 mM tris-Cl (pH 7.6)], and incubated at 37°C for 30 min. Samples were electrophoresed through a 12% SDS–polyacrylamide gel electrophoresis (PAGE) gel. Western blotting was performed with the alkaline phosphatase detection method by using the rat antiserum to BlaI as the primary antibody (*31*). The antiserum was raised in Sprague-Dawley rats injected with purified GST-BlaI fusion protein.

protein, BlaR1, only a few copies of which are present in the membrane. Binding promotes rapid autocatalytic cleavage of BlaR1, which appears to be a prometalloprotease. The activated metalloprotease either directly cleaves BlaI or promotes or participates with one or more cofactors in BlaI cleavage to generate an 11-kD fragment containing the DNA binding domain and a 3-kD fragment containing the dimerization domain. Repression is reversed by converting the BlaI monomer to a form that is incapable of dimerizing and binding. Loss of BlaI from its intergenic operator sites allows transcription of *blaZ*. β-Lactamase is then expressed, resulting in resistance. Because BlaR1 once cleaved can no longer transmit signal, intact BlaR1 must be continually generated in order to detect antibiotic in the environment, which explains why its production is also up-regulated. As the antibiotic concentration decreases, BlaR1 is no longer autoactivated, BlaI is no longer cleaved, and equilibrium shifts back to the intact repressor, which can again dimerize, bind DNA, and turn the system off. The simplest model for signal transduction would involve direct cleavage of BlaI by BlaR1. However, Cohen and Sweeney (*25*) have reported that a putative third chromosomal regulatory element, *blaR2*, was also involved in β-lactamase induction. Our results do not rule out the participation of such an additional element or elements.

Regulation by a transmembrane signal transmitted by sequential proteolytic events has not been described in bacteria. The β-lactamase regulatory system differs from two bacterial systems in which protease activity is involved in gene regulation or transmembrane signaling (*26–28*). The *E. coli* FtsH membrane metalloprotease is a constitutively expressed enzyme that degrades the heat-shock transcriptional factor σ^{32}, which affects transcription of several genes (*27*). There is, however, no sensor component of this system. The *Bacillus subtilis* membrane protease SpoIIGA (*28*) perhaps most closely resembles β-lactamase gene regulation. SpoIIGA protease activity is increased in the presence of an endogenously produced ligand and converts the transcription factor precursor pro-σ^E into its active form. However, SpoIIGA activation does not involve proteolysis. Thus, regulation of β-lactam resistance in staphylococci occurs through a specific pathway that may offer potential targets for drug development.

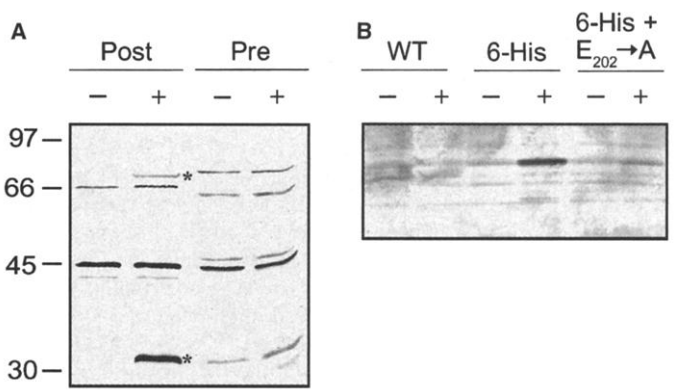

Fig. 2. (**A**) Western blot of BlaR1 in membranes of strain COL631, a transformant of the methicillin-resistant strain COL into which pCH631 has been introduced (*24*). Each lane indicates the growth of cells under noninducing (–) or inducing (+) conditions. BlaR1 was detected by a rabbit antiserum, which was prepared in New Zealand rabbits by intradermal immunization with a 14–amino acid synthetic peptide identical to the sequence S^{281}HSFNGKKSLLKRR^{294} of the BlaR1 cytoplasmic domain. Post indicates postimmunization serum, and Pre indicates preimmune serum. Numbers at the left indicate the position of migration of molecular weight markers (in kilodaltons). β-Lactamase induction and immunoblotting was performed as described in Fig. 1. (**B**) Western blot with monoclonal antibody to His^6 in whole-cell lysates of RN4220 transformants, uninduced (–) and induced (+). WT indicates the RN4220 (pCH2278) transformant containing wild-type *bla*. Lanes 6-His are a transformant with His^6 tagged onto the COOH-terminus of BlaR1 (*15, 16*) and wild-type H^{201}EXXH motif. Lanes 6-His + E_{202}→A are a transformant with His^6-tagged BlaR1 plus this substitution mutation in its HEXXH motif. BlaR1 was detected by immunoblotting with monoclonal antibody to His^6 (Invitrogen).

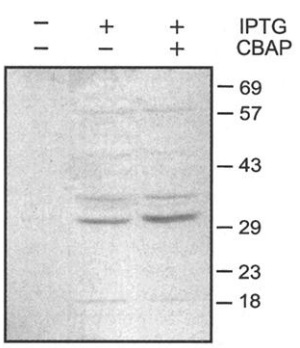

Fig. 3. Western blot of His^6-tagged BlaR1 peptides purified from *E. coli* strain BL21(DE3) (Invitrogen). *blaR1* with His^6 tagging sequence and its intact ribosome binding site was amplified by PCR from the *S. aureus* RN4220 transformant described in Fig. 2 and cloned downstream of the T7 promoter into pBluescript SK^- (Stratagene). The T7 promoter with tagged *blaR1* was amplified by PCR and recloned into a low-copy-number plasmid, pACYC184 (New England BioLabs, Beverly, Massachusetts), which was used to transform *E. coli* strain DH5α. The resulting plasmid, p184R6H, was used to transform BL21(DE3). The BL21(DE3) (p184R6H) transformant was grown to an optical density at 600 nm of ~0.5, and BlaR1 expression was induced with IPTG in the presence or absence of CBAP (10 μg/ml) for 1 hour. Cell lysate equivalent to 10 ml of culture was subjected to metal affinity precipitation by using the Talon Metal beads (Clontech). Beads were boiled for 5 min in SDS sample buffer, and samples were loaded on an SDS-PAGE gel for immunoblotting with monoclonal antibody to His^6 (Invitrogen). Numbers at the right indicate the position of migration of molecular weight markers (in kilodaltons). Lanes indicate the presence (+) or absence (–) of IPTG and CBAP in the growth medium. Relative amounts of protein were determined by scanning densitometry.

References and Notes

1. B. J. Hartman, A. Tomasz, *J. Bacteriol.* **158**, 513 (1984).
2. W. M. M. Kirby, *Science* **99**, 452 (1944).
3. H. de Lencastre, B. L. de Jonge, P. R. Matthews, A. Tomasz, *J. Antimicrob. Chemother.* **33**, 7 (1994).
4. H. F. Chambers, M. Sachdeva, *J. Infect. Dis.* **161**, 1170 (1990).
5. W. Tesch, C. Ryffel, A. Strassle, F. H. Kayser, B. Berger-Bachi, *Antimicrob. Agents Chemother.* **34**, 1703 (1990).
6. S. J. Rowland, K. G. Dyke, *EMBO J.* **8**, 2761 (1989).
7. T. Kobayashi, Y. F. Zhu, N. J. Nicholls, J. O. Lampen, *J. Bacteriol.* **169**, 3873 (1987).
8. K. Hiramatsu, *Microbiol. Immunol.* **39**, 531 (1995).
9. V. K. Sharma, C. J. Hackbarth, T. M. Dickinson, G. L. Archer, *J. Bacteriol.* **180**, 2160 (1998).
10. P. D. Gregory, R. A. Lewis, S. P. Curnock, K. G. Dyke, *Mol. Microbiol.* **24**, 1025 (1997).
11. C. J. Hackbarth, H. F. Chambers, *Antimicrob. Agents Chemother.* **37**, 1144 (1993).
12. G. L. Archer, D. M. Niemeyer, J. A. Thanassi, M. J. Pucci, *Antimicrob. Agents Chemother.* **38**, 447 (1994).
13. K. Kuwahara-Arai, N. Kondo, S. Hori, E. Tateda-Suzuki, K. Hiramatsu, *Antimicrob. Agents Chemother.* **40**, 2680 (1996).
14. K. Hardt *et al.*, *Mol. Microbiol.* **23**, 935 (1997).
15. A. N. Vallejo, R. J. Pogulis, L. R. Pease, *PCR Methods Appl.* **4**, S123 (1994).
16. *S. aureus* strain RN4220 (*29*) was used for all transformation experiments, unless otherwise indicated. Plasmid pRN5542 (*30*) was used as the *S. aureus* cloning vector. Plasmid pCH2278 is the entire *bla* region of *S. aureus* strain 67-0 cloned into pRN5542 (*11, 24*). Specific mutations were introduced into *bla* according to the following procedures. The entire *bla* region (*blaI-blaR1-blaZ*) was cloned into Sal I and Hinc II sites of pBluescript SK^- to produce pCH227. The 1.0-kb Hind III–Hinc II fragment containing *blaZ* and a 13-nucleotide fragment of NH_2-terminal *blaR1* was recloned into pBluescript to yield pSK1.0. Desired mutations of *blaR1* or *blaI* were introduced by manipulation of the remaining 2.2-kb Hind III–Sal I fragment by overlapping-extension polymerase chain reaction (PCR) using KlenTaq enzyme (Clontech, Palo Alto, CA) (*15*). This 2.2-kb fragment was amplified as a PCR product with Hind III sites at both ends by using the following primers: P1 (5′-TATCCTAAGCTTCATATGTATTATGTTTG-3′) and P4 (5′-GGCTAAGTTATTAATAATGAGCATAGTAAGCTTTTGTT-3′). c-Myc or His^6 encoding sequence was incorporated in primers when necessary. Primer sets for individual mutations were as follows: BlaR1 H201A mutation, $P2R_{H/A}$ (5′-ATATATAATATTGGCTGAATATGCTCATGC-3′) and $P3R_{H/A}$ (5′-GCATGAGCATATTCAGCCAATATTATATAT-3′); BlaR1 E202A mutation, primers $P2R_{E/A}$ (5′-ATATATAATATTGCATGCATATGCTCATGC-3′) and $P3R_{E/A}$ (5′-GCATGAGCATATGCATGCAATATTATATAT-3′); BlaR1 R293A mutation, $P2R_{R/A}$ (5′-GTCATTACTCAAAAGAGCATTAATTAATATAAAAGAAGCC-3′) and $P3R_{R/A}$ (5′-GGCTTCTTTTATATTAATTAATGCTCTTTTGAGTAATGAC-3′); and BlaI N101A, F102A mutation, $P2I_{AA}$ (5′-AAGTTTAGTGCTGGCTGCTGCGAAAAATGAAG-3′) and $P3I_{AA}$ (5′-CTTCATTT-

TTCGCAGCAGCCAGCACTAAACTT-3'). Each 2.2-kb Hind III fragment generated from PCR mutagenesis was then cloned into the Hind III site of pSK1.0 to obtain the mutant plasmid in *E. coli* strain DH5α. The restoration of the entire *bla* region in the correct orientation was confirmed by restriction mapping. This mutant plasmid was ligated into Sma I–digested *S. aureus* plasmid pRN5542 for transformation into *S. aureus* strain RN4220. NH_2-terminal amino acid sequence was determined by Edman degradation reaction by the University of California at San Francisco Biomolecular Resource Center.

17. G. I. Evans, G. K. Lewis, G. Ramsey, V. M. Bishop, *Mol. Cell. Biol.* **5**, 3610 (1985).
18. GST-BlaI fusion protein expression and purification were performed with the GST Gene Fusion System (Pharmacia Biotech). BlaI-GST and BlaR1-His^6 were constructed with overlapping-extension PCR (*15*) in the context of an otherwise wild-type *bla* region. A culture of recombinant *S. aureus* strain RN4220 was grown in the presence of CBAP (10 μg/ml) to induce expression of the fusion product. Cells were harvested and mechanically disrupted by glass beads in a cell homogenizer. Cleared lysates containing BlaI-GST were subject to the purification procedure by using a GST protein purification kit (Clontech). BlaR1-His^6 fusion protein was purified with the Talon Metal column purification kit (Clontech).
19. Single-letter abbreviations for the amino acid residues are as follows: A, Ala; C, Cys; D, Asp; E, Glu; F, Phe; G, Gly; H, His; I, Ile; K, Lys; L, Leu; M, Met; N, Asn; P, Pro; Q, Gln; R, Arg; S, Ser; T, Thr; V, Val; W, Trp; and Y, Tyr.
20. β-Lactamase activity was assessed with Nitrocephin discs, according to manufacturer's instructions (Becton-Dickinson).
21. N. M. Hooper, *FEBS Lett.* **354**, 1 (1994).
22. W. Jiang, J. S. Bond, *FEBS Lett.* **312**, 110 (1992).
23. C. Marie-Claire, B. P. Roques, A. Beaumont, *J. Biol. Chem.* **273**, 5697 (1998).
24. C. J. Hackbarth, C. Miick, H. F. Chambers, *Antimicrob. Agents Chemother.* **38**, 2568 (1994).
25. S. Cohen, H. M. Sweeney, *J. Bacteriol.* **95**, 1368 (1968).
26. J. S. Parkinson, *Cell* **73**, 857 (1993).
27. T. Tomoyasu *et al.*, *EMBO J.* **14**, 2551 (1995).
28. A. E. Hofmeister, A. Londono-Vallejo, E. Harry, P. Stragier, R. Losick, *Cell* **83**, 219 (1995).
29. B. Kreiswirth *et al.*, *Nature* **227**, 680 (1983).
30. R. Novick, *Methods Enzymol.* **204**, 587 (1991).
31. E. Harlow, D. Lane, *Antibodies: A Laboratory Manual* (Cold Spring Harbor Laboratory Press, Cold Spring Harbor, NY, 1988).

32. This research was supported by NIH/National Institute of Allergy and Infectious Diseases grants AI4005804 (C.J.H.) and AI46610 (H.F.C.). We are grateful for the critical review of the manuscript by P. Rosenthal and J. Ernst.

22 August 2000; accepted 15 January 2001

Recovery of Infectious Ebola Virus from Complementary DNA: RNA Editing of the GP Gene and Viral Cytotoxicity

Viktor E. Volchkov,[1,2]* Valentina A. Volchkova,[1] Elke Mühlberger,[1] Larissa V. Kolesnikova,[1] Michael Weik,[1] Olga Dolnik,[1] Hans-Dieter Klenk[1]

To study the mechanisms underlying the high pathogenicity of Ebola virus, we have established a system that allows the recovery of infectious virus from cloned cDNA and thus permits genetic manipulation. We created a mutant in which the editing site of the gene encoding envelope glycoprotein (GP) was eliminated. This mutant no longer expressed the nonstructural glycoprotein sGP. Synthesis of GP increased, but most of it accumulated in the endoplasmic reticulum as immature precursor. The mutant was significantly more cytotoxic than wild-type virus, indicating that cytotoxicity caused by GP is down-regulated by the virus through transcriptional RNA editing and expression of sGP.

Ebola virus (EBOV) is a highly dangerous pathogen causing hemorrhagic fever in humans and nonhuman primates. Mortality rates up to 90% and the lack of measures to prevent the disease classify this virus at biosafety level P4 (*1*). Together with Marburg virus (MBGV), it forms the family Filoviridae (*2*), a group of enveloped, nonsegmented, negative-stranded RNA viruses. The EBOV genome is 18,959 nucleotides (nt) in length and is transcribed into eight major subgenomic mRNAs that encode seven structural proteins and one nonstructural protein. Four of these—NP, VP35, VP30, and the catalytic subunit L of the RNA polymerase—are constituents of the ribonuleocapsid (*2*). VP40 and VP24 are matrix proteins. GP is a membrane glycoprotein that is located at the surface of EBOV-infected cells and forms the spikes on virions. Expression of GP, which is encoded by two overlapping reading frames, requires the insertion of a non–template-coded adenosine residue by a mechanism of transcriptional RNA editing (*3*, *4*). Most (about 80%) GP mRNAs are not edited, and they direct synthesis of the nonstructural glycoprotein sGP, which is secreted from EBOV-infected cells. GP and sGP are identical at their NH_2-terminal ends (295 amino acids) but differ at the COOH termini owing to the use of different reading frames. Surface GP presumably mediates virus entry by receptor binding and membrane fusion and is a determinant of cell tropism (*5*, *6*). Proteolytic cleavage of GP may play a role in pathogenesis (*7*). It has recently been reported that recombinant GP induces cell disruption and cytotoxicity and that it may therefore be a determinant of pathogenicity (*8*, *9*). Significant amounts of sGP can be detected in sera of patients suffering from EBOV hemorrhagic fever, which supports the notion that sGP also plays an important role in pathogenesis (*10*). However, MBGV, which causes disease symptoms similar to those of EBOV, expresses only GP from a single open reading frame (*11*, *12*). GP levels are low in cells infected with MBGV, although editing does not occur in this case. Therefore, the roles of transcriptional editing and of sGP in EBOV replication and pathogenesis are not well understood. The present study was undertaken to elucidate these problems.

A cDNA clone encoding the complete antigenome of the Mayinga strain of EBOV subtype Zaire (*13*), was constructed from three overlapping cDNA segments of approximately 6000 base pairs (bp) (KSN-4, KSS-25, and KSL-23), each generated from a plasmid library described elsewhere (*14*–*16*). As a marker for the rescue of recombinant EBOV (recEBOV), two nucleotide mutations at a unique Sal I restriction site were introduced into the antigenomic cDNA by means of site-directed mutagenesis (*17*). This clone, which contained the authentic editing site, was designated pFL-$EBOVe^+$. To recover recEBOVe^+, a BHK-21 cell line (BSR T7/5) stably expressing T7 polymerase under the control of a cytomegalovirus promoter (*18*), was cotransfected with pFL-$EBOVe^+$ and four plasmids encoding the nucleocapsid proteins NP, VP35, VP30, and L (*19*, *20*). A typical cytopathic effect (CPE) in the form of several foci of rounded cells was observed in cell culture dishes between 6 and 9 days after transfection. To amplify rescued virus, culture supernatants from BSR T7/5 cells were inoculated onto Vero E6 cells, where recombinant virus induced easily visible CPE 4 to 6 days after infection. When any of the plasmids expressing NP, VP35, VP30, or L was omitted, CPE was not observed in either BSR T7/5 cells or in subsequent passages on Vero E6 cells, which supports the previous observation that NP, VP35, and L are essential for

[1]Institut für Virologie, Philipps-Universität, Robert-Koch-Strasse 17, 35037 Marburg, Germany. [2]University Claude Bernard Lyon-1, Filovirus Laboratory, 21 Avenue Tony Garnier, 69365 Lyon Cedex 07, France.

*To whom correspondence should be addressed. E-mail: viktor.volchkov@ens-lyon.fr